Cellular/Molecular

Uncoupling Proton Activation of Vanilloid Receptor TRPV1

Sujung Ryu,* Beiying Liu,* Jing Yao,* Qiang Fu,* and Feng Qin
Department of Physiology and Biophysical Sciences, State University of New York at Buffalo, Buffalo, New York 14214

Multimodal gating is an essential feature of many TRP ion channels, enabling them to respond to complex cellular environments. TRPV1, a pain receptor involved in nociception at the peripheral nerve terminals, can be activated by a range of physical and chemical stimuli (e.g., capsaicin, proton, and heat) and further sensitized by proinflammatory substances. How a single receptor achieves this multiplicity of functionality is poorly understood at the molecular level. Here, we investigated the structural basis of proton activation of TRPV1. Chimeric channels between rTRPV1 and the low pH-insensitive homolog TRPV2 were constructed by systematically exchanging the extracellular domains and were characterized using whole-cell recording in transiently transfected HEK293 cells. Two discrete domains, one involving the pore helix and the other the S3–S4 linker, were found crucial for direct activation of the channel by low pH. Single residue mutations in either domain (T633A/V538L) abrogated the proton-evoked current while preserving the capsaicin and heat responses and their potentiation by mildly acidic pH. Both residues exert a gating effect through hydrophobic interactions. Our results unravel novel information on the structural basis of channel function, and support the existence of discrete domains for multimodal gating of the channel. In view of the resemblance of the pore of TRPV1 to KcsA, our findings also provide evidence on the pore helix as an active component in channel gating in addition to its role in ion permeation.

Key words: **capsaicin channel; TRP channel; thermal receptor; multimodal gating; pore loop; pain**

Introduction

Local tissue acidosis occurs during infection, inflammation, or ischemia, and contributes to pain and hyperalgesia in disease states. The extracellular pH can drop to as low as pH 6, altering the activity of many receptors and ion channels in the primary afferents. There is compelling evidence that the vanilloid receptor TRPV1 mediates the slow, sustained proton responses in these neurons (Bevan and Docherty, 1993). Infusion of acidified physiological solution produces an intense burning pain (Steen and Reeh, 1993), similar to intradermal application of capsaicin (Simone et al., 1989). Mice lacking TRPV1 are impaired in sensation of severe acidification, and their cultured dorsal ganglion neurons show reduced proton responses (Caterina et al., 2000; Davis et al., 2000).

TRPV1 responds to an acidic attack in two ways. Moderate acidification sensitizes its responses to other stimuli such as capsaicin and heat (Petersen and Lamotte, 1993; Martenson et al., 1994; Baumann et al., 1996; Kress et al., 1996; Tominaga et al., 1998). Severe acidification directly activates the channel (Bevan and Yeats, 1991; Tominaga et al., 1998). The two effects of low pH on the channel appear mechanistically distinct. The potentiation of capsaicin response by low pH involves allosteric modulation of capsaicin binding and stabilization of opening (Ryu et al., 2003). A glutamic residue (E600) on the extracellular side of the fifth transmembrane segment is crucial for the low pH potentiation (Jordt et al., 2000). An antibody to the region inhibits the low pH activity of the channel (Klionsky et al., 2006). Another acidic residue, E648, located in the linker between the selectivity filter and the sixth transmembrane domain, was proposed to mediate the direct response to low pH (Jordt et al., 2000). The residue as well as two other pore acidic residues, E636 and D646, were also suggested to specifically contribute to capsaicin response without affecting proton or thermal sensitivity (Welch et al., 2000). Similar findings were reported for residues on the pore-aligning segment where mutation tended to affect the capsaicin activity more profoundly (Kuzhikandathil et al., 2001). An emerging notion from these studies is that the channel may undergo distinct conformational changes in response to different stimuli.

In the present study, we focused on the structural basis of proton activation of TRPV1. Exploiting the low pH-insensitive homolog TRPV2 as a template, we constructed chimeras of TRPV1 by exchanging the extracellular segments with the cognate regions of TRPV2. Two sites were found essential, one involving the pore helix and the other the S3–S4 linker. Following with site-directed mutagenesis, we further identified single critical residue in each domain, T633 in the pore helix and V538 in the S3–S4 linker. Mutation of either residue removed the proton currents while leaving normal responses to capsaicin and low pH potentiation. Both residues appeared to be involved in hydrophobic interactions, most likely mediating the coupling of proton sensor activation to gate opening. Our data suggest the existence of structural domains specific for proton activation of the channel. Given the physical separation of the two sites, they also indicate a global conformational change evoked by protonation.

Received May 21, 2007; revised Sept. 10, 2007; accepted Sept. 16, 2007.

This work was supported by National Institutes of Health Grants R01-RR11114 and R01-GM65994. We thank Dr. Fred Sachs for critical reading of this manuscript.

*S.R., B.L., J.Y., and Q.F. contributed equally to this work.

Correspondence should be addressed to Dr. Feng Qin, 335 Cary Hall, University at Buffalo, Buffalo, NY 14214. E-mail: qin@buffalo.edu.

DOI:10.1523/JNEUROSCI.2324-07.2007

 0270-6474/07/2712797-11$15.00/0

Materials and Methods

Mutagenesis and expression. The wild-type (WT) rat TRPV1 and TRPV2 cDNAs were generously provided by David Julius (University of California, San Francisco, San Francisco, CA) (Caterina et al., 1997, 1999). Mutations and chimeras were generated using the overlap-extension PCR method as described previously (Liu et al., 2004). Fragments of residues that were exchanged between TRPV1 and TRPV2 were as follows (TRPV1/TRPV2): P456–T476/P415–L436 for the first extracellular loop between S1 and S2, S532–M541/M492–L501 for the second loop between S3 and S4, L585–L664/L547–L627 for the pore loop, 601–611/E561–N671 for the turret, Y627–C634/Y590–S597 for the pore helix, and D646–V667/E609–V631 for the S6-linker. All recombinant constructs were confirmed by restriction enzyme digestion and by DNA sequence analysis. Capped cRNA was synthesized using the mMessage mMachine kit (Ambion, Austin, TX). The final cRNA was resuspended in RNase-free water to ~1 ng/nl and kept at −80°C.

The HEK293 cell lines were used for whole-cell measurement. Cells were maintained in DMEM plus 10% fetal bovine serum (HyClone Laboratories, Logan, UT) with 1% penicillin/streptomycin, incubated at 37°C in 5% CO_2, and transfected at a confluence of ~80% using the standard calcium phosphate precipitation method as described previously (Liu et al., 2004). Either GFP (green fluorescent protein) or human CD8 lymphocyte antigen (0.5 μg/0.2 ml) was cotransfected as surface markers. Electrophysiological recordings took place 10–28 h after transfection. For cells cotransfected with CD8, antibody-coated beads were used to visually identify the transfected cells (Dynabeads M450 CD8; Dynal, Lake Success, NY). For visualization of the expression of TRPV1 and its mutants, the channels were tagged with EGFP (enhanced green fluorescent protein) at the C-terminal, and the plasma membrane was delineated by coexpression of the phosphatidylinositol-4,5-bisphosphate (PIP2)-binding construct phospholipase C-δ (PLC-δ) pleckstrin homology (PH) domain tagged with monomeric red fluorescent protein (mRFP) (kindly provided by Christopher Kearn, University of Washington, Seattle, WA).

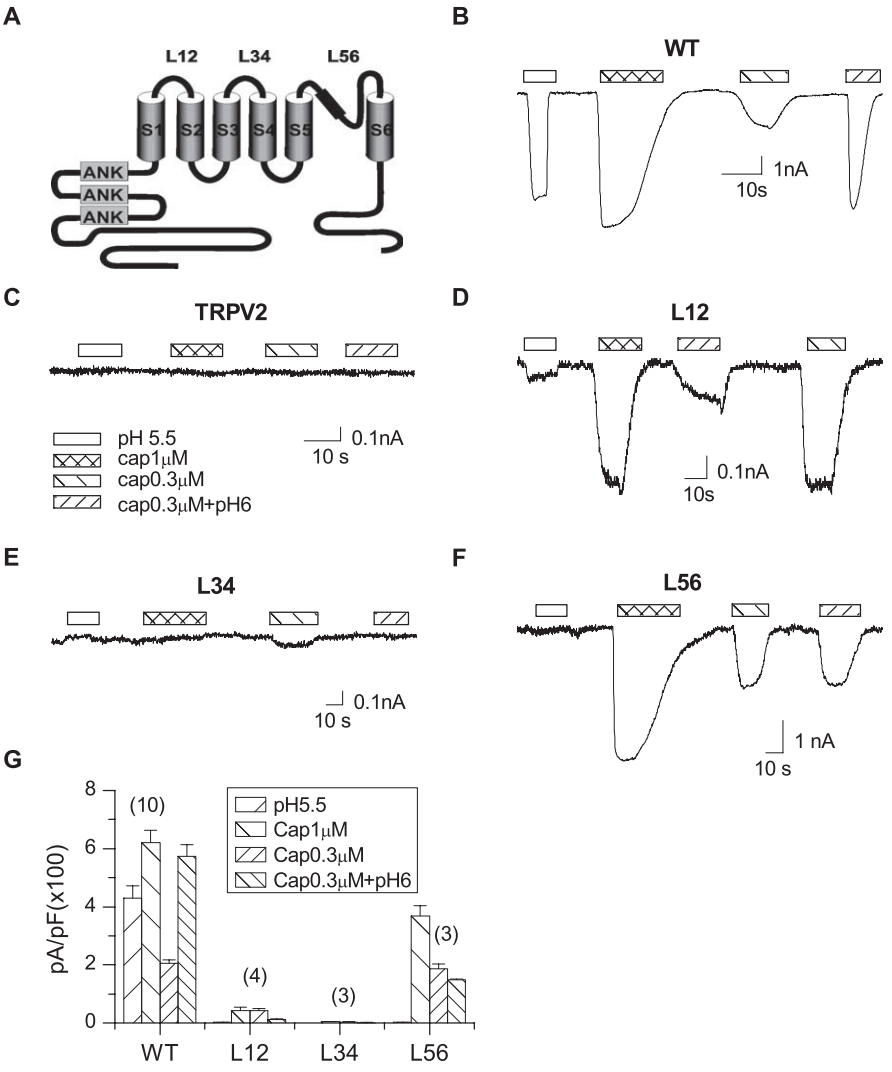

Figure 1. Screen of extracellular segments for proton sensitivity of TRPV1. ***A***, Putative membrane topology showing the three extracellular linker regions, represented by L12, L34, and L56, respectively. ***B–F***, Representative traces of whole-cell currents from the wild-type TRPV1, wild-type TRPV2, and the TRPV1 chimeras containing replacement of each of the extracellular linkers by the cognate segment of TRPV2. The currents were evoked by 1 μM capsaicin or pH 5.5. The potentiation effect of low pH was tested by application of 0.3 μM capsaicin alone and in combination with pH 6. Holding potential $V_h = -60$ mV. ***G***, Current density of the chimera channels compared with that of the wild-type TRPV1. The labels over the bars indicate the number of recordings. Data are expressed as mean ± SEM.

The oocyte expression system was used for single-channel recordings (Hui et al., 2003). *Xenopus laevis* oocytes were surgically removed, enzymatically separated using collagenase, and hand-selected 1 or 2 d after harvesting for microinjection of the channel cRNA. Typically, each oocyte received 10–30 ng of cRNA. The injected oocytes were incubated in ND96 solution supplemented with 2.5 mM sodium pyruvate, 100 U/ml penicillin, and 100 μg/ml streptomycin at 18°C for 2–7 d before use.

Electrophysiology. Conventional whole-cell and excised patch-clamp recording methods were used. Patch pipettes were fabricated from borosilicate glass (Sutter Instrument, Novato, CA), coated with Sylgard (Dow-Corning, Midland, MI), and fire-polished to a resistance between 0.5 and 2.5 MΩ for whole-cell recordings, and 6 and 10 MΩ for single-channel recordings. Currents were amplified using an Axopatch 200B amplifier (Molecular Devices, Foster City, CA) and recorded through a BNC-2090/MIO acquisition system (National Instruments, Austin, TX) using custom-designed software. Whole-cell recordings were typically filtered at 1 kHz and sampled at 5 kHz, and single-channel recordings were filtered at 10 kHz and sampled at 25 kHz. Currents were evoked from a holding potential of either −60 mV (inward) or +60 mV (outward). All experiments except those on heat activation were conducted at room temperature (21–25°C).

The bath solution for whole-cell recording from HEK 293 cells contained the following (in mM): 150 NaCl, 5 EGTA, 10 HEPES, pH 7.4 (adjusted with NaOH). The internal pipette solution contained the following (in mM): 140 CsCl, 10 HEPES, 1 EGTA, pH 7.4 (adjusted with CsOH). The bath and pipette solutions for single-channel recording in oocytes were symmetrical and contained 100 mM Na-gluconate and 10 mM NaCl instead of 150 mM NaCl, and other components were the same as the bath solution for HEK 293 cells. Exchange of external solutions was performed using a gravity-driven perfusion system with manually controlled solenoid valves (ALA Scientific Instruments, Westbury, NY). The perfusion solutions were the same as the bath solutions except for appropriate agonists. For recordings from HEK 293 cells under low pH conditions, the solution also contained 50 μM amiloride as a blocker for the native ASIC channels. Buffers used for low pH solutions were MES [2-(*N*-morpholino)ethanesulfonic acid] for pH 3.5–6.5 and HEPES for

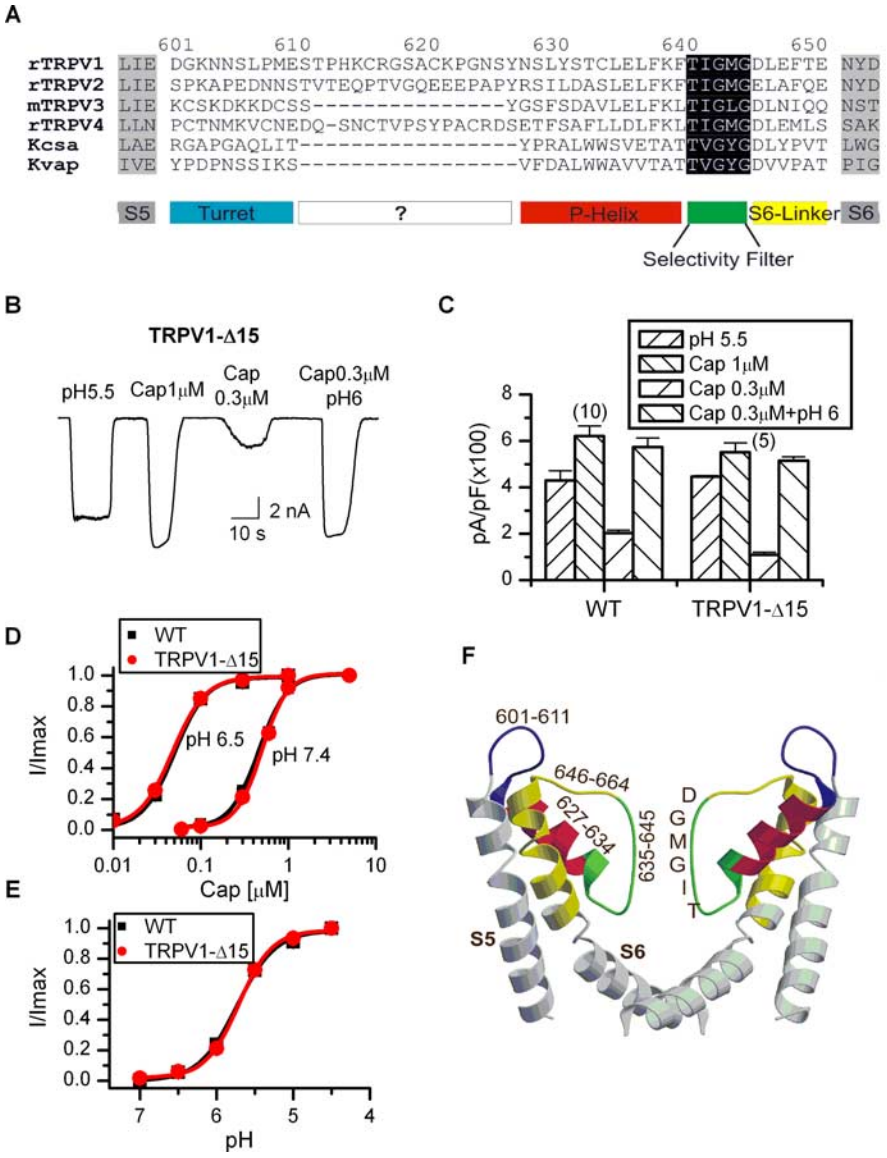

Figure 2. Delineation of functional domains in the pore loop of TRPV1. ***A***, Alignment of the pore sequence of TRPV1 with other TRPV channels and K^+ channels. TRPV1 and TRPV4, but not TRPV3, contain an extra region of 15 residues (T612–S626) between the turret and the pore helix. The rest of the sequences could be reasonably aligned with those of K^+ channels, most notably in the region of the selectivity filter. ***B***, Deletion of the 15-residue region between the turret and the pore helix did not affect channel function. ***C***, Comparison of the current density between the wild-type TRPV1 and the deletion mutant TRPV1-Δ15, showing similar maximum responses under various test conditions. Error bars indicate SEM. ***D***, Dose–response curves of capsaicin for the wild type and the deletion mutant. WT, $EC_{50} = 0.48 \pm 0.03$ μM, $n_H = 2.6 \pm 0.3$ at pH 7.4; $EC_{50} = 0.05 \pm 0.004$ μM, $n_H = 2.5 \pm 0.3$ at pH 6.5; TRPV1-Δ15, $EC_{50} = 0.5 \pm 0.02$ μM, $n_H = 2.8 \pm 0.3$ at pH 7.4; $EC_{50} = 0.05 \pm 0.002$ μM, $n_H = 2.4 \pm 0.1$ at pH 6.5. ***E***, Dose–response curves of low pH. $pK_a = 5.7 \pm 0.04$ for WT and 5.7 ± 0.02 for TRPV1-Δ15. ***F***, A homology model for the pore structure of the deletion mutant TRPV1-Δ15, constructed from the structure of KcsA using the Swiss-Model and the Swiss-Pdb Viewer software (www.expasy.ch/swissmod/SWISS-MODEL.html) (Guex and Peitsch, 1997) based on the alignment shown in ***A***.

pH 7.0–7.4. Solutions were titrated to their nominal pH at room temperature (21–25°C). Capsaicin was purchased from Fluka (Sigma, St. Louis, MO). Capsazepine was from Precision Biochemicals (Vancouver, British Columbia, Canada). All other chemicals were from Sigma. Capsaicin and capsazepine were dissolved in 100% ethanol to make a 1 mM stock solution, stored at 4°C, and diluted into the recording solution at appropriate concentrations before experiment (0.001–0.1% final ethanol).

Temperature control. Cells were placed in a narrow, rectangular chamber. Heat stimulus was applied by exchanging the entire content of the recording bath through an inline SH-27B heater powered by a TC-324B temperature controller (Warner Instruments, Hamden, CT). The actual temperature of the recording was monitored during an experiment using a miniature thermocouple (Warner Instruments) placed near the pipette tip. The temperature drop between the tip and the thermocouple was <0.5°C throughout the entire tested temperature range (40–50°C) (Liu et al., 2003). The reported temperature corresponds to the readout of the thermocouple without corrections.

Results

Extracellular loops are functionally important

Previous studies on the proton sensitivity of TRPV1 have focused on the extracellular acidic residues (Jordt et al., 2000; Welch et al., 2000). To obtain a more complete understanding of the process, we took a chimera approach and investigated the extracellular domains systematically. TRPV2 is a homolog of TRPV1 with 46% identity in the primary amino acid sequence (Caterina et al., 1999) and is not activated by the external low pH. Both channels are predicted to have a membrane topology of six transmembrane segments (S1–S6) and a pore loop between S5 and S6 (Fig. 1*A*). Because protons only activate TRPV1 extracellularly, we constructed chimeric channels by replacing each of the extracellular loops of TRPV1, namely, L12, L34, and L56, with the corresponding segment of TRPV2. The resultant chimeras were designated as TRPV1-L12, -L34, and -L56, respectively.

The function of the chimeric channels was tested by the whole-cell recording in transiently transfected HEK293 cells. Figure 1 compares their responses to capsaicin and low pH with those of the wild-type channels. Both capsaicin and low pH evoked large inward currents in the wild-type channels at saturating concentrations, and their simultaneous application at low concentrations resulted in a synergistic increase in response (Fig. 1*B*). Because the acidic pH actually suppresses the unitary inward conductance of TRPV1 (Baumann and Martenson, 2000; Ryu et al., 2003), the increase in the open probability (P_o) was more profound than suggested by the mean current. The chimeric channels were considerably different. In particular, the replacement of the pore region between S5 and S6 abrogated the activity at pH 5.5 and the synergistic interaction between capsaicin and low pH (Fig. 1*F*,*G*). The capsaicin response at pH 6 showed a slight decline presumably because of the proton block of permeation. In contrast to the loss of low pH responses, capsaicin continued to evoke a significant current although somewhat smaller than the wild type (Fig. 1*F*,*G*). Exchange of the linker between S3 and S4, on the other

hand, produced no detectable current in response to either capsaicin or low pH (Fig. 1*E*), although the swapped region is the shortest among the three linkers (10 residues). The TRPV1-L12 chimera of the first loop between S1 and S2 remained functional and showed a reduced low pH current (Fig. 1*D*). But its response to capsaicin was also decreased and remained potentiated by mildly acidic pH. Notably, capsaicin at 0.3 μM evoked a current as large as at 1 μM, suggesting an increase in the apparent sensitivity. The linker thus has a broad impact on channel functions. Because of the relatively specific loss of proton sensitivity in the pore loop chimera, we first focused on the pore region to determine what features were important for proton activation.

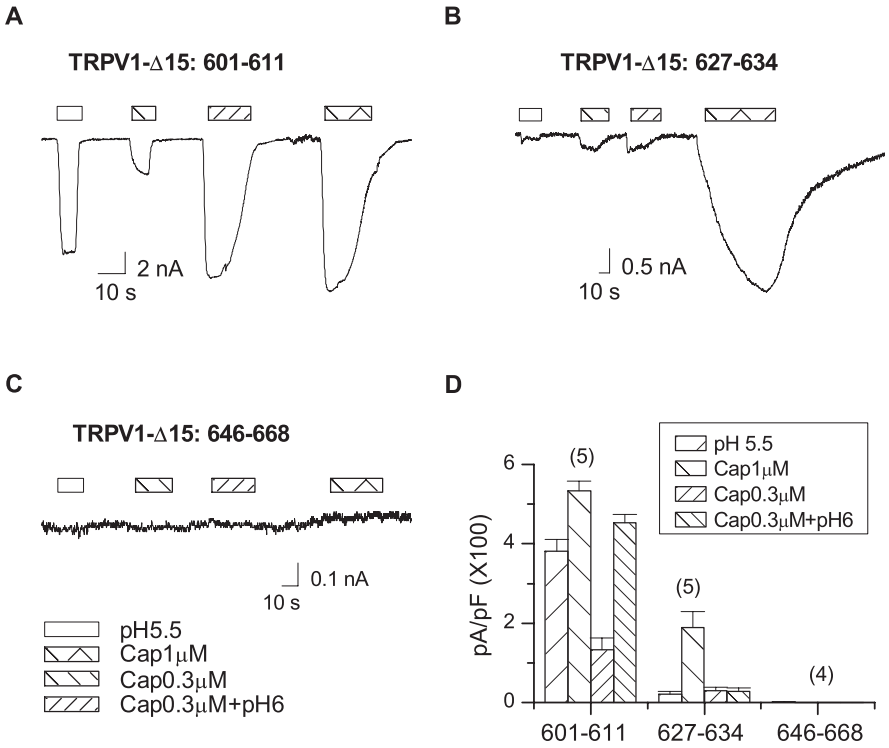

Figure 3. Screen of pore domains for proton activation of TRPV1-Δ15. The turret, the pore helix, and the S6-linker of TRPV1-Δ15 were each swapped with the corresponding segments of TRPV2, respectively. ***A–C***, Whole-cell recordings from the chimera channels evoked by 1 μM capsaicin, 0.3 μM capsaicin, pH 5.5, and the combination of 0.3 μM capsaicin and pH 6. Holding potential $V_h = -60$ mV. The exchange of the pore helix eliminated both the proton-evoked currents and the potentiation of capsaicin responses by low pH. It also slowed down the activation by capsaicin. The swap of the turret did not significantly alter channel functions, whereas the replacement of the S6-linker was deleterious. ***D***, Average responses of the chimera channels evoked by different stimuli. Error bars indicate SEM.

A minimal pore channel

The pore loop of TRPV1 has several features consistent with a molecular architecture similar to the KcsA, including a similar signature sequence of TIGMG, which is conserved among all TRPV channels, and a salt bridge between E636 and K639 (Garcia-Martinez et al., 2000), whose locations are compatible with an α-helical secondary structure preceding the segment of the signature sequence. We aligned the sequence of the pore of TRPV1 to that of KcsA and found significant homology on the C-terminal half. However, the homology was less clear in the region between S5 and the selectivity filter, where the sequence of TRPV1 is considerably longer (Fig. 2*A*). We first examined whether this region confers any TRPV1-specific function. In comparison with other TRPV channels, we noticed that TRPV3 has a pore sequence comparable in length to that of KcsA, whereas TRPV1 and TRPV4 contain an extra stretch of 15 residues between the turret and the selectivity filter (Fig. 2*A*). Based on the finding, we constructed a deletion mutant without the 15 residues (T612–S626), named TRPV1-Δ15. Figure 2*B* illustrates the whole-cell responses of the mutant channel to various stimuli. Capsaicin and low pH remained effective, producing similar maximum currents to the wild type (Fig. 2*C*). The mutant also showed a wild-type dose–response relationship for capsaicin and low pH (Fig. 2*D*,*E*). The removal of the 15 residues did not appear to alter channel functions.

Because of its wild-type responses, we used the deletion mutant in our subsequent construction of pore loop chimeras. The mutant offers some advantages over the wild-type TRPV1. It has a minimal pore and thus simplified the search for critical residues. More importantly, its pore domain has a sequence length comparable with KcsA, thereby allowing for a more accurate sequence alignment and the construction of a homology model for the pore structure (Fig. 2*F*). Based on the model, we were then able to delineate the four domains of the pore, the turret, the pore helix, the selectivity filter, and the S6-linker (Fig. 2*A*,*F*). The role of each of these domains in proton sensitivity was then further investigated.

Pore helix mediates proton activation

Except the selectivity filter, which is conserved among TRPV1–4, we exchanged the other three functional domains in TRPV1-Δ15 with the counterparts of TRPV2. For the turret chimera, we also excluded E600, which is known to be required for proton potentiation of the channel. Of the three chimeras, the pore helix swapping showed a diminished low pH response (Fig. 3*B*). The capsaicin activation also became considerably slower, but the steady-state current remained large. In addition, mild acidification (pH 6) did not augment capsaicin responses below saturation (0.3 μM). The swap of the pore helix thus caused a selective loss of proton sensitivity of the channel. In contrast to the pore helix swap, the exchange of the turret preserved the wild-type responses to both capsaicin and low pH (Fig. 3*A*). The S6-linker chimera, on the other hand, exhibited no detectable activity with either capsaicin or low pH. Fluorescence experiments confirmed that the chimera was similarly expressed as the WT channels on the plasma membranes, which were delineated by coexpression of the mRFP-tagged, PIP2-binding construct PH PLC-δ (data not shown). A structural defect is thus likely responsible for the functional loss of the chimera.

T633 as a critical residue

The pore helix of TRPV1 and TRPV2 differs mainly in the N terminus. We mutated each of the different residues in the region in TRPV1-Δ15 to that of TRPV2 (except L630 which has a similar counterpart Ile in TRPV2). A single residue, T633, was uncovered. Substitution of the residue by alanine

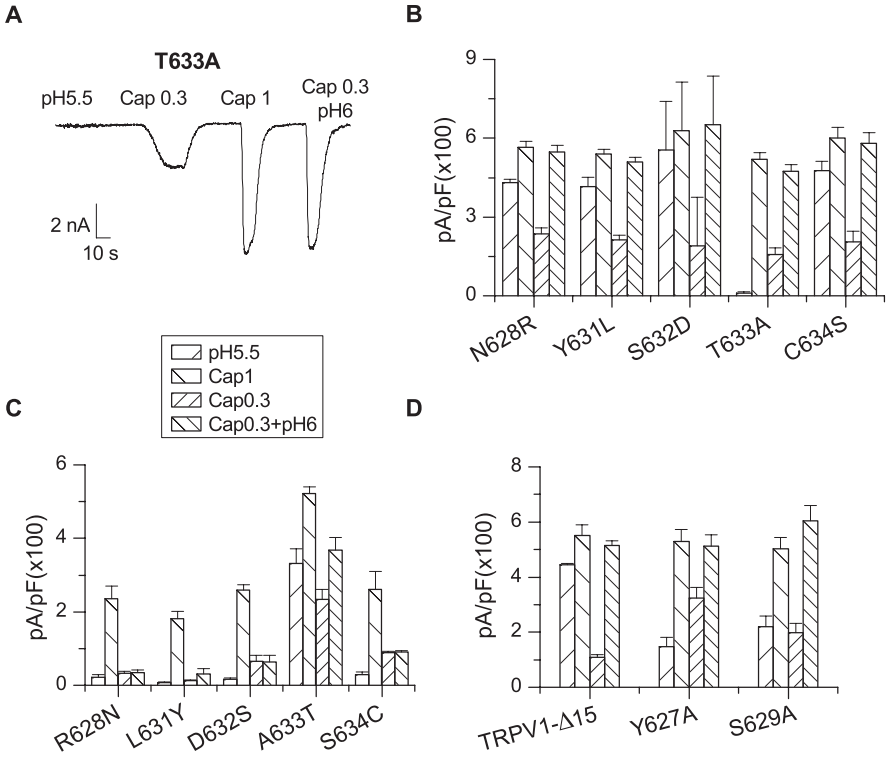

Figure 4. Identification of critical residues in the pore helix for proton activation of TRPV1. ***A***, A representative whole-cell recording of the T633A mutant. Holding potential $V_h = -60$ mV. ***B***, Results from the forward mutations in TRPV1-Δ15. The residues in the pore helix of TRPV1-Δ15 were each mutated to the cognate residues of TRPV2. Substitution of T633 by alanine caused a specific loss of low pH currents while retaining normal activity to capsaicin and potentiation by low pH. Mutation of other residues did not alter channel function significantly. ***C***, Results from the recovery mutations in the pore helix chimera. The mutation of A633 to T resulted in a significant recovery of the low pH response. The capsaicin peak current and its potentiation by low pH were also improved compared with those of the chimera channel. ***D***, Screen of other pore helix residues near T633 that are conserved between TRPV1 and TRPV2. They were substituted by alanine in TRPV1-Δ15. Error bars indicate SEM.

abrogated low pH-activated currents as observed in the pore helix chimera (Fig. 4*A*,*B*). But, unlike the latter, the T633A mutant exhibited normal capsaicin responses including rapid activation kinetics and large steady-state currents (Fig. 4*A*). Furthermore, the potentiation by low pH was also retained despite the loss of the low pH sensitivity for direct activation. In the presence of 50 μM amiloride to block the background ASIC channels, the mean residual current of T633A at pH 5.5 was ~2% of the 1 μM capsaicin response, as opposed to ~81% in TRPV1-Δ15. The mutation reduced the proton response by >97% even if the mutant carried all the residual current. To the contrary, the change of the capsaicin response was <5% (519 ± 27 pA/pF for the mutant and 551 ± 40 pA/pF for TRPV1-Δ15). Thus, the residue appeared to specifically affect the proton activation of the channel.

The mutations of other residues had minimal consequences, leaving capsaicin and low pH responses mostly intact. These include radical perturbations such as the charge mutations N628R and S632D, suggesting that these residues are probably exposed to the aqueous phase. Such an arrangement would be consistent with their positions in a helix, which renders T633 facing away from the aqueous phase, making it accessible to interaction with other residues.

Recovery mutations in the pore helix chimera also support a role for T633 in proton activation. In these experiments, each of the different residues on the pore helix in the chimera channel was restored to the wild type, one at a time. Among all mutations, only the recovery of T633 gave rise to a substantial response to low pH (Fig. 4*C*). The other mutations retained the chimeric phenotypes, with virtually no pH current, slow capsaicin activation, and no potentiation by acidic pH.

We also examined two conserved residues on the N-terminal end of the pore helix, namely Y627 and S629. They were each mutated to alanine in TRPV1-Δ15. Both mutants were functional and produced relatively normal responses to capsaicin when applied either alone or in combination with mildly acidic pH (Fig. 4*D*). The mutants were also activated by low pH directly, albeit a slightly smaller maximal current than TRPV1-Δ15. The data suggest that these residues may contribute to, but do not play a pivotal role in the proton activation of TRPV1 as T633 does.

T633 affects channel gating

Because of the proximity of T633 to the permeation pathway of the channel, we examined whether the residue exerted its effect on gating or conductance. Single-channel recordings were acquired from excised membrane patches of oocytes perfused with either low pH or capsaicin. In TRPV1-Δ15, pH 5.5 evoked long bursts of activity in which the openings were separated by brief closures (Fig. 5*A*). The T633A mutant instead showed rare spike-like openings (Fig. 5*B*). The mutation drastically slowed the opening rate at low pH. The significant shortening of the open time also suggests that the mutation destabilizes the open conformation of the channel.

Whole-cell dose–response relationships of the mutant also support a gating effect of the residue on the low pH activation. The capsaicin response was similar to that of the wild-type channel at both normal pH and pH 6.5 (Fig. 5*C*). Furthermore, lowering pH resulted in a similar leftward shift of the dose–response curve. In contrast, the dose–response relationship of low pH was markedly suppressed (Fig. 5*D*). Over the entire accessible low pH range (pH 7.4–3.5), T633A produced virtually no detectable current (Fig. 5*D*), consistent with the rare activity observed in single-channel recording.

Effects on heat activation

The effect of T633 on heat sensitivity was studied at the whole-cell level. The ambient temperature of the bath solution was changed by inline heating to ~50°C over ~1 min (Fig. 5*E*). For the wild-type channel, a large current was evoked once the temperature was raised >40°C. The steady-state current was comparable with that evoked by 1 μM capsaicin (95%) (Fig. 5*E*,*F*). The activation threshold, which was measured at the temperature at which the current reached 10% of its maximum, was ~43°C. The T633A mutant exhibited a weaker response, reaching ~32% of the 1 μM capsaicin current (Fig. 5*F*). However, in contrast to the change of the peak activity, the thermal activation threshold coincided with that of the wild type (~42°C) (Fig. 5*F*) and remained sensitized by lowering pH (T633A, 33°C at pH 6.0; WT, 35°C at pH 6.5). The mutation thus affected primarily the maximal response of

heat activation. In many patches, we observed a large irreversible reduction of the capsaicin current after heating. We do not know whether this apparent loss of the functional channels was responsible for the reduction of the heat-activated currents, or alternatively, the residue was involved in heat activation. Regardless of the underlying mechanisms, the effect of the mutation on the heat response was less dramatic than on the low pH response, arguing that the two processes were different.

Side-chain property of T633

To understand what feature of T633 makes it so sensitive, we systematically mutated the residue to others including Y, R, Q, N, L, K, E, D, V, S, and A, which span both polarity and size. The results are summarized in Figure 6*A*. The hydrogen-bonding capability appeared nonessential. Substitutions with polar residues such as Q, N, and Y or the charged residues R, K, E, and D all resulted in nonfunctional channels. The T-to-S mutation was functional, but with a significant reduction in low pH current and a slow activation by capsaicin. However, the T-to-V mutation preserved the wild-type responses in all aspects (Fig. 6*B*). Substitution by leucine with a larger hydrophobic side chain became nonfunctional again. Together, these results suggest that T633 is involved in functional interactions in a compact hydrophobic environment. The size of the side chain at the position is crucial. Replacing T by A, a smaller side chain, was able to preserve the capsaicin response while abrogating the low pH activation, and a larger side-chain substitution at the position, on the other hand, became deleterious.

S3–S4 linker

Our initial screen of the extracellular linkers suggested possible roles of the S3–S4 loop in channel functions. We further examined whether the region is involved in proton activation of the channel. Because the linker is relatively short, we mutated all residues, one at a time, to the counter residues in TRPV2 (Fig. 7). Several mutations were effective, including K535E, E536W, V538L, and A539P. These residues were clustered around the center of the loop, and the mutations appeared to predominantly impact the proton responses. This is particularly evident with V538L, which resulted in no detectable current at pH 5.5 while retaining >93% of the wild-type peak capsaicin response. The capsaicin response of E536W was also reduced; however, the mutation, as well as K535E and A539P, involved substantial changes in the side-chain property. Such substitutions could produce nonlocal perturbations on the channel structure and consequently nonspecific phenotype changes. Common to all these mutations is the significant, consistent reduction of the low pH current, suggesting that the region plays an important role in proton activation. Mutations at the two ends of the S3–S4 linker showed little effects on either capsaicin or low pH responses. These include S532M, Q533E, S540L, and M541L. In addition, unlike the swap of the entire region, no single mutation sufficed to ablate the channel function, suggesting that a collective interaction from multiple residues probably contributed to the chimeric phenotype.

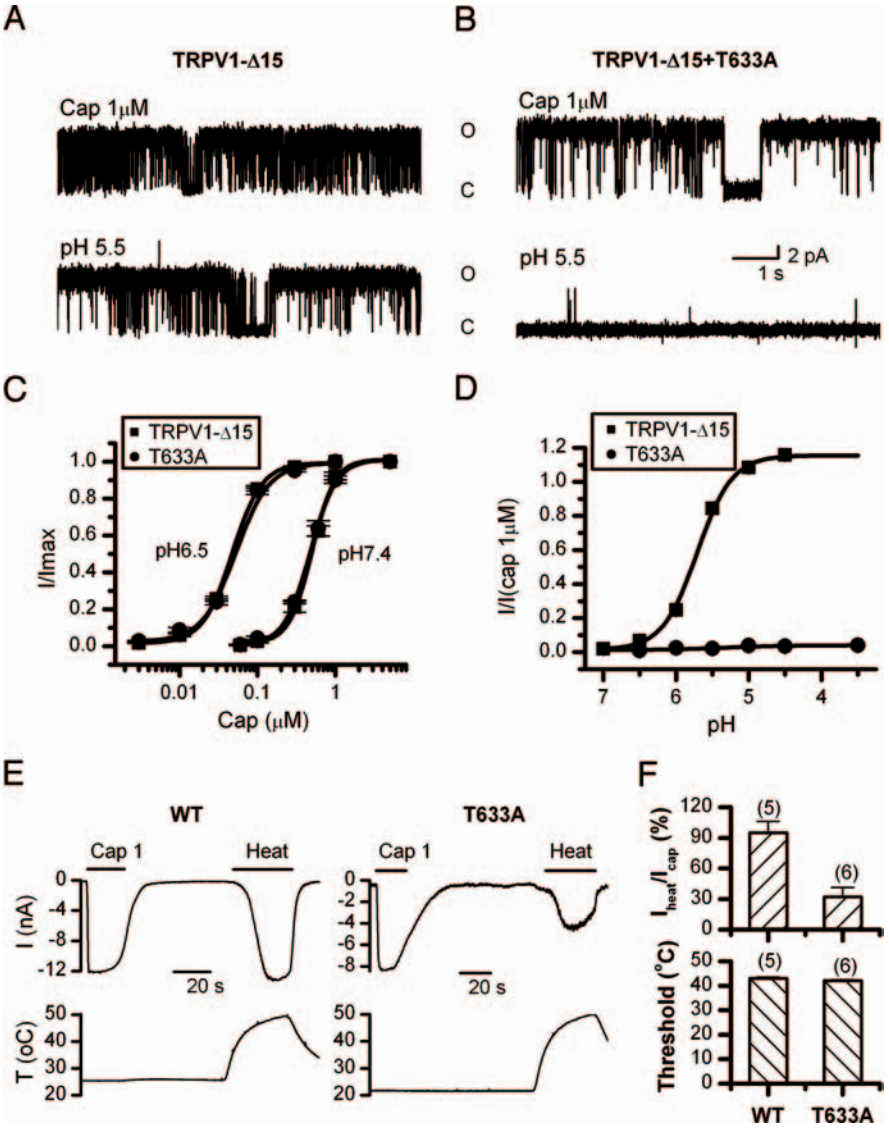

Figure 5. Functional characterization of the T633A mutant. ***A***, ***B***, Single-channel currents of TRPV1-Δ15 and T633A evoked by capsaicin (1 μM) or low pH (5.5). Currents were recorded from excised membrane patches of oocytes at +60 mV. The mutation retained high P_o for capsaicin, but profoundly suppressed low pH-evoked opening. ***C***, Dose–response curves of capsaicin at pH 7.4 and 6.5. The fitting by Hill's equation resulted in the following: TRPV1-Δ15, $EC_{50} = 0.49 \pm 0.02$ μM, $n_H = 2.8 \pm 0.3$ for pH 7.4, and $EC_{50} = 0.05 \pm 0.002$ μM, $n_H = 2.4 \pm 0.1$ for pH 6.5; T633A, $EC_{50} = 0.48 \pm 0.02$ μM, $n_H = 2.7 \pm 0.2$ for pH 7.4, and $EC_{50} = 0.05 \pm 0.004$ μM, $n_H = 2.5 \pm 0.3$ for pH 6.5. ***D***, Dose–response curves of low pH. The fitting gave a pK_a value of 5.71 ± 0.02 for TRPV1-Δ15. The response for the mutant channel was too small for a reliable fitting. ***E***, Representative traces of heat-evoked currents of the wild-type TRPV1 and the T633A mutant in comparison with the responses from 1 μM capsaicin in the same cells. The bottom traces illustrate the heat stimulation protocol. Recordings were from transiently transfected HEK293 cells held at −60 mV. ***F***, Comparison of the peak response and temperature threshold of heat activation between the wild type and TRPV1-Δ15-T633A. The peak response was normalized to the maximal current evoked by 1 μM capsaicin from the same cells. The activation threshold was determined as the temperature at which the current reached 10% of its maximum. The mutation reduced the current size without significantly altering the temperature threshold. Error bars indicate SEM.

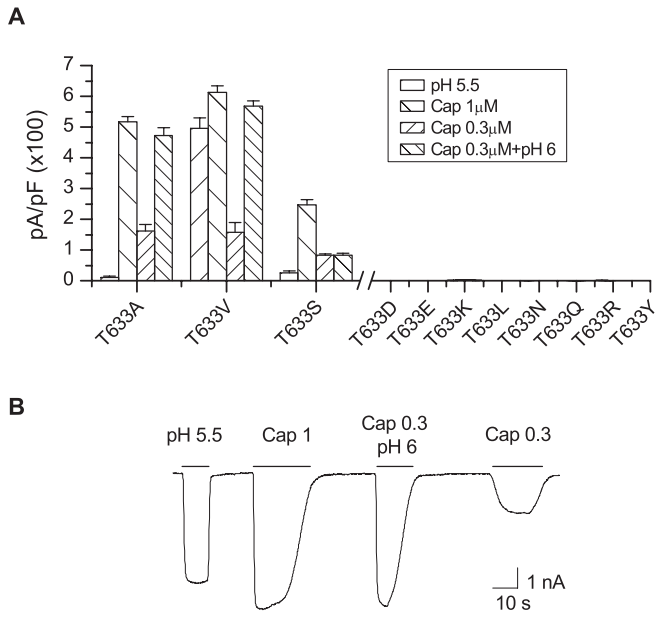

Figure 6. Side-chain property at position 633. ***A***, Average current responses to 1 μM capsaicin, pH 5.5, 0.3 μM capsaicin, and 0.3 μM capsaicin plus pH 6 for various substitutions introduced at T633. The T-to-V mutation retained normal responses to all stimuli, whereas substitutions with a larger side-chain size showed no detectable activity. Error bars indicate SEM. ***B***, A representative current trace from the T633V mutant showing its wild-type-like responses.

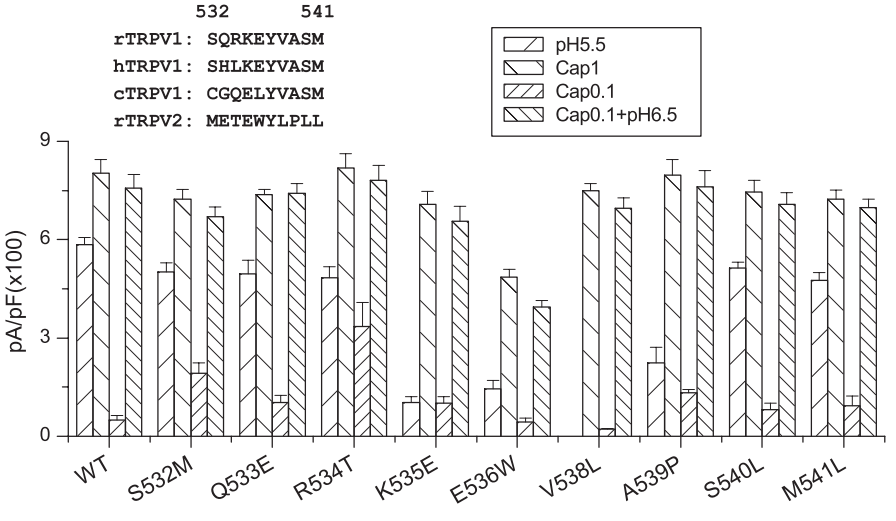

Figure 7. Identification of critical residue in the S3–S4 loop. Each residue in the loop of the wild-type TRPV1 was mutated to the counter residue of TRPV2. The peak responses of the mutants to 1 μM capsaicin, pH 5.5, 0.3 μM capsaicin, and 0.3 μM capsaicin plus pH 6.5 were summarized. The inset shows the amino acid sequences of the region of the TRPV1 orthologs and rat TRPV2. The mutation V538L resulted in a selective loss of the low pH current while leaving intact the capsaicin response and its potentiation by low pH. Error bars indicate SEM.

V538 mediates proton activation

To further determine the specific function of the S3–S4 linker, we studied the mutant V538L in more detail. Figure 8 compared the dose–response relationships of capsaicin between the mutant and the wild-type channels. They were superimposed at both neutral and mildly acidic pH (6.5), respectively. Best fitting by Hill's equation resulted in EC_{50} and n_H of 0.47 ± 0.03 μM and 2.58 ± 0.3 for WT at pH 7.4, 0.49 ± 0.02 μM and 2.62 ± 0.28 for V538L at pH 7.4, 0.05 ± 0.004 μM and 2.54 ± 0.28 for WT at pH 6.5, and 0.05 ± 0.001 μM and 2.58 ± 0.11 for V538L at pH 6.5. The mutant was close to the wild type in both EC_{50} and the cooperativity. Furthermore, lowering pH produced a comparable shift of the dose–response curve. Combined with the similar peak currents in the previous measurement, the results suggest that the capsaicin activation and its potentiation by low pH were not altered by the mutation at the macroscopic level.

The relationship of the pH dose–response showed a marked reduction in the maximal activity (Fig. 8*C*). The data were normalized by the 1 μM capsaicin current from the same patches. Whereas the wild-type channel produced a maximal current at pH 4.5 approximately the same as the capsaicin response, the mutant gave rise to only ~8% at pH 3.5, corresponding to >90% suppression of the low pH activity. Also unlike T633A, which showed no measurable pH current over the entire pH range, V538L exhibited a titration curve with a consistently increasing trend as pH was lowered (pK_a = 5.7 ± 0.03 for WT and 4.6 ± 0.1 for V538L). This residual current was persistent despite thorough wash after capsaicin perfusion and was also observed in the first patch from a fresh dish, suggesting that it was not attributable to capsaicin contamination. It appears that the mutation weakened, but did not disrupt the pH gating completely.

The V538L mutant also exhibited a robust heat response. The current was rapidly activated >40°C and appeared to reach saturation ~50°C (Fig. 8*D*). The mean peak current was comparable with that of 1 μM capsaicin from the same cells, similar to the observations with the wild-type channels (Fig. 8*F*). This contrasts with T633A, which showed a reduced maximum heat current. The temperature threshold at 10% activation was also similar to that of the wild type (WT, 42.9 ± 0.5°C; V538L, 42.2 ± 0.4°C). In addition, the heat response remained to be potentiated by low pH (Fig. 8*E*). At pH 6.5, the threshold was reduced to ~36°C, whereas the maximum current was similar to the 1 μM capsaicin response. These results further argue for a specific role of the residue in proton activation of the channel.

Side-chain property of V538

Figure 9 summarizes the mutagenesis results from a series of mutations introduced at V538. The function of the channel appeared quite sensitive to perturbations at the position. Even a relatively conservative substitution by alanine abrogated the low pH currents and also reduced the capsaicin activity. Further reducing the size of the side chain with a substitution by glycine resulted in nonfunctional channels. It appeared that the local structure of the channel lacks rigidity to tolerate a smaller side chain at the position. However, the size of the side chain was not the only determinant for the function of the residue. Replacement by isoleucine, which has the same volume as leucine, recovered a small but significant portion of the low pH activity. The data appeared to consist of two populations, one similar to the wild type and the other to V538L, as if the local structure of the channel existed in some metastates. Finally, the threonine substitution, which preserved the side-chain size, did not confer the wild-type responses either. Together, these data indicate that multiple aspects of the side chain including both volume and steric hindrance are important for the function of the residue.

Specificity to proton gating

The mutagenic effects of the residues (T633 and V538) could be interpreted by two different mechanisms; one is a specific effect on proton activation, the other a more general effect on both proton and capsaicin responses. The two hypotheses could be more explicitly illustrated by an allosteric model in scheme I, assuming an equilibrium constant K_0 for the intrinsic opening between C_0 and O_0 and two allosteric coupling factors α and β for capsaicin and proton binding, respectively, as depicted in the submodels in schemes II–V. A specific effect on proton activation corresponds to a change in either the protonation step or the coupling strength β, whereas a general effect argues for a change in the intrinsic opening equilibrium constant K_0. The latter could be the case if the energetic coupling of capsaicin binding to the gate is so strong that the mutant could still retain a full response.

We resorted to quantitative modeling to differentiate the two hypotheses. We assumed that the mutation altered the intrinsic gating ($K_0 \rightarrow K_1$) and calculated the expected changes of the maximum open probability of the mutant channel for various stimuli. The maximal responses were determined from schemes II–V, which were reductions of the full model under the conditions of no ligand or saturating concentrations. For wild-type channel, the maximal P_o values were given by the following:

$$P_o^{(0)} = \frac{1}{1+\frac{1}{K_0}},\ P_o^{(C)} = \frac{1}{1+\frac{1}{\alpha K_0}},$$

$$P_o^{(H)} = \frac{1}{1+\frac{1}{\beta K}},\ \text{and}$$

$$P_o^{(CH)} = \frac{1}{1+\frac{1}{\alpha\beta K_0}},$$

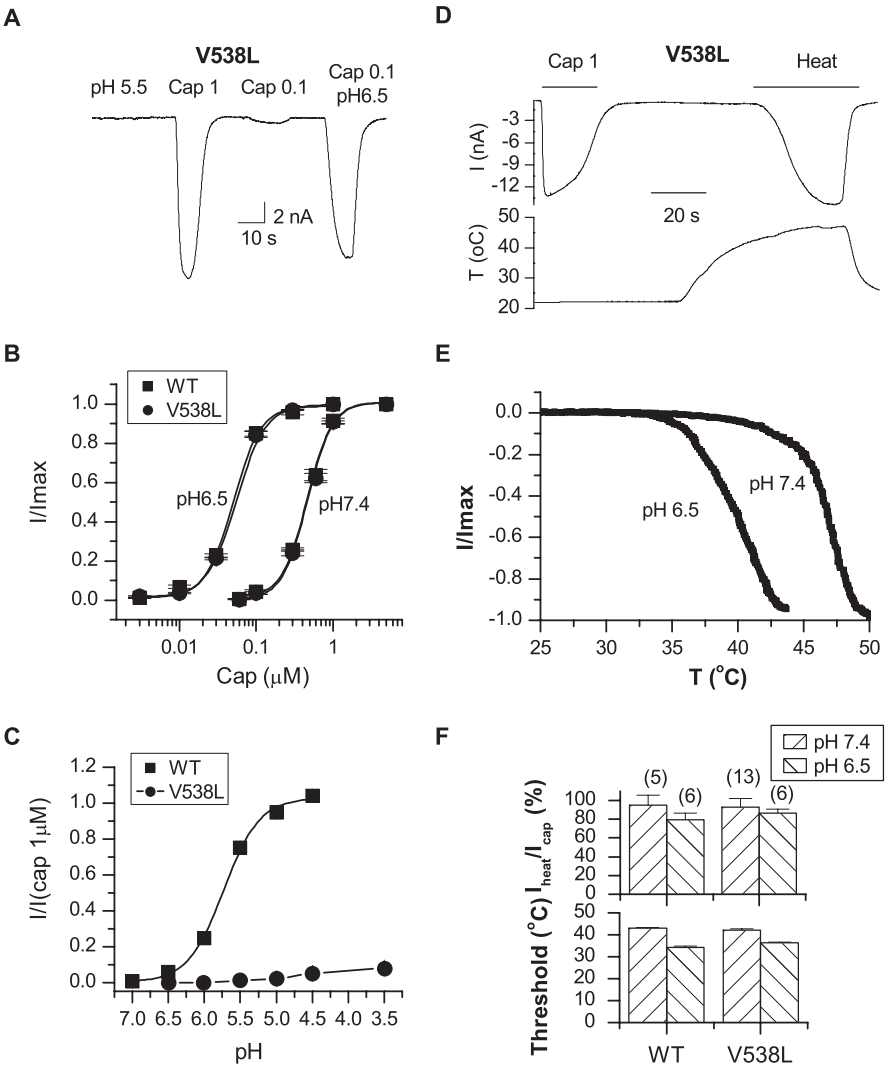

Figure 8. Functional role of V538. ***A***, A whole-cell current trace of V538L in response to capsaicin, low pH, and their combination. Whereas capsaicin activated a wild-type response, low pH produced no detectable current. Data were recorded from transiently transfected HEK293 cells held at −60 mV. ***B***, Dose–response curves of capsaicin alone and in combination with pH 6.5. Best fitting by Hill's equation resulted in the following: WT, $EC_{50} = 0.48 \pm 0.03$ μM, $n_H = 2.6 \pm 0.3$ for pH 7.4; $EC_{50} = 0.05 \pm 0.004$ μM, $n_H = 2.54 \pm 0.28$ for pH 6.5; V538L, $EC_{50} = 0.49 \pm 0.02$ μM, $n_H = 2.62 \pm 0.28$ for pH 7.4; $EC_{50} = 0.05 \pm 0.001$ μM, $n_H = 2.58 \pm 0.11$ for pH 6.5. ***C***, Dose–response curves of low pH of the wild-type channel and V538L; $pK_a = 5.73 \pm 0.03$ for WT and 4.63 ± 0.07 for V538L. ***D***, Heat-evoked whole-cell current of V538L. Capsaicin (1 μM) was applied at the beginning for the comparison of peak responses. The bottom trace shows the temperature change. Holding potential $V_h = -60$ mV. ***E***, Current–temperature relationships of V538L at the normal (pH 7.4) and acidic pH (6.5). ***F***, Comparison of the peak current (normalized by the 1 μM capsaicin response from the same cells) and the activation threshold of temperature between the wild type and V538L. Both the maximum current and the activation threshold of the mutant remained similar to those of the wild-type channels. Error bars indicate SEM.

where the superscripts were for spontaneous opening, capsaicin, low pH, and the combination of the two, respectively. The mutant responses were similar except that K_0 was replaced by the altered equilibrium constant K_1. Because the variables K_0, α, β, and K_1 were not directly observable, we used three other experimentally accessible measurements to parameterize the model, namely, r_H (the reduction of the low pH current of the mutant relative to the wild type), θ (the ratio of the low pH current of the wild type to its capsaicin response), and λ (the capsaicin response of the wild type relative to the spontaneous activity of the channel). The original parameters K_0, β, and K_1 were then derived from the new variables according to the following:

$$K_0 = \frac{1-\frac{\lambda}{\alpha}}{\lambda - 1},\ \beta = \frac{\theta}{1-\theta+\frac{1}{\alpha K_o}} \cdot \frac{1}{K_0}$$

$$\text{and } K_1 = \frac{1}{\beta\left(\frac{1}{r_H}-1\right)+\frac{1}{r_H K_0}}.$$

Figure 10 shows the predicted maximal responses of the mutant channel (top panel) and the changes relative to the wild type (bottom panel). They were plotted as a function of α, the coupling strength of capsaicin binding. The other three vari-

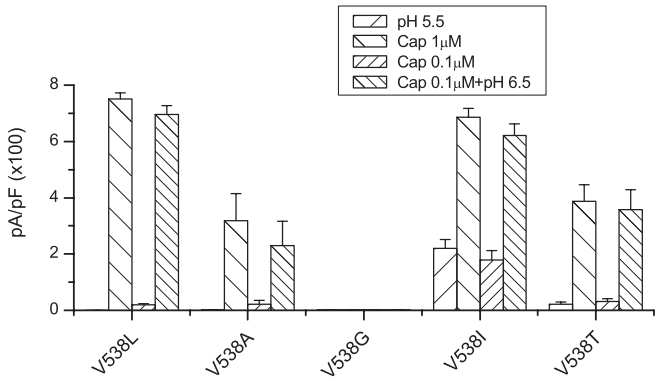

Figure 9. Side-chain property at position 538. The peak current responses to 1 μM capsaicin, pH 5.5, 0.1 μM capsaicin, and 0.1 μM capsaicin plus pH 6.5 from various mutations introduced at V538 were plotted. The leucine and isoleucine substitutions resulted in different low pH responses albeit similar capsaicin currents. Data were recorded from transiently transfected HEK293 cells at −60 mV. Error bars indicate SEM.

ables were assumed to be $r_H = 90\%$, $\theta = 80\%$, and $\lambda = 1000$. The values of r_H and θ were taken from the preceding data. The value of λ was estimated assuming an average capsaicin response of 10 nA and a spontaneous activity of 10 pA. The latter was determined from the reduction of the leakage current after application of 1 μM ruthenium red. Although these estimates were conservative and did not take account of the smaller unitary current of low pH than capsaicin, the resultant capsaicin P_o of the mutant was already <20% of the wild type over a wide range of α values (the response to the combination of capsaicin and low pH remained high). Single-channel recordings suggest a maximal P_o of capsaicin ~0.8 (Hui et al., 2003; Ryu et al., 2003). This P_o mapped to $\alpha \approx 6000$ (marked by the dotted vertical line), which was in the range of $r_C < 20\%$. In the other words, the model predicted that the capsaicin response would be reduced by at least 80% if the proton response changed by 90%. This is contrary to our apparent observation, which showed <10% change in capsaicin response. The simulation thus argues against the assumption that the mutation altered K_0 and supports instead a specific effect of these residues on proton gating.

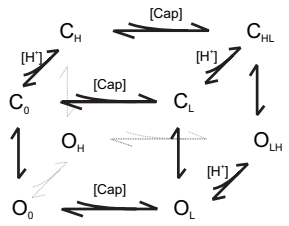

Scheme I

Scheme II

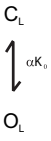

Scheme III

Scheme IV

Scheme V

Discussion

We identified two functional sites for the gating of TRPV1, one involving the pore helix and the other the linker between S3 and S4 segments. Mutations in either site ablated proton activation of the channel while retaining the capsaicin and heat responses as well as the potentiation by the mildly acidic pH. The T633A mutant reached a peak capsaicin current ~95% of the wild type and a potentiated capsaicin response ~92%. The V538L mutant produced a capsaicin response ~93% of the wild type at the normal pH and ~92% at pH 6.5. In addition to the peak responses, the capsaicin dose–response relationships and the heat activation threshold were also similar to the wild type. Although T633 was located in the pore region, single-channel recordings showed that a gating defect, rather than a conductance change, was mainly responsible for the mutagenesis effects.

Neither T633 nor V538 is titratable. Although there are charged residues in their vicinity, the neutralization of these residues did not produce large spontaneous activity in the mutant channels. The two sites that harbor these residues, the pore helix and the S3–S4 linker, are thus unlikely involved in proton binding. Instead, they appear more likely to mediate the energetic transduction between proton sensor activation and gate opening. The involvement of V538 also underscores the importance of the peripheral domains of the channel for proton activation. This extends the previous findings on the acidic residues in the pore region (Jordt et al., 2000; Welch et al., 2000), and suggests a global conformational change evoked by protonation. The latter is consistent with the pharmacological data, which shows that capsazepine, a competitive inhibitor of capsaicin, inhibits both capsaicin- and proton-evoked currents in rat TRPV1. To this end, the proton activation of the channel is analogous to the capsaicin activation, involving both the peripheral domains (S1–S4) and the pore region. It is remarkable that, despite the large and possibly overlapping conformational changes, the molecular pathways for the two activations remain segregated at multiple positions downstream of their apparently different binding sites.

It has been proposed that the two proton effects, the potentiation and direct activation of the channel, are mediated by different mechanisms (Jordt et al., 2000). In the present study, we observed that the mutations at either T633 or V538 retained normal potentiation of the capsaicin responses. The result is consistent with such a model and suggests that these residues are likely involved in the direct activation by low pH only. With the disruption of the proton activation by either T633A or V538L, no current was detected at pH 5.5, suggesting that the potentiation mechanism alone did not activate the channel. It also implies that the potentiation did not lower the heat activation threshold below the ambient temperature (25°C). The potentiation effect likely reaches saturation before the full activation by low pH. However, the allosteric interaction between capsaicin and proton gating predicts a secondary cross-sensitization between the two stimuli, which should continue until the channel is fully activated. The mutants reported in the present study will be useful for further differentiating the two sensitization effects of low pH in the future.

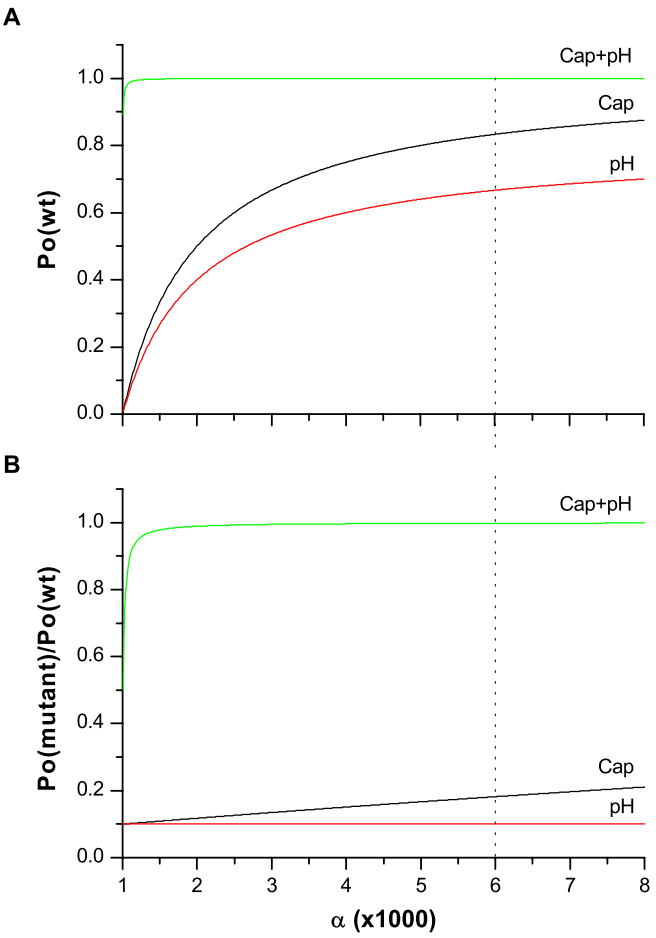

Figure 10. A quantitative analysis of a MWC allosteric model showing that a mutation that produces a selective loss of the low pH activity as observed is mechanistically specific to proton activation. The bottom panel shows the expected change of the maximum P_o for the three stimuli: capsaicin (r_C), low pH (r_H), and their combination (r_{CH}). The simulation was based on the model in scheme I, and the maximum P_o values were calculated using the reduced models in schemes II–V under the assumption of $r_H = 90\%$, $\lambda = 1000$, and $\theta = 80\%$, where $r_H \equiv P_o^{(mutant)}(H^+)/P_o^{(wt)}(H^+)$, $\lambda \equiv P_o(\text{cap})/P_o(\text{spontaneous})$, and $\theta \equiv P_o(H^+)/P_o(\text{cap})$. The abscissa, α, represents the strength of the allosteric coupling of capsaicin binding to gate opening and is plotted as a variable. For comparison, the maximum P_o of the wild-type channel is plotted on the top. The dotted line locates the value of α for a typical capsaicin $P_o = \sim 0.8$. The mutation is assumed to alter the intrinsic opening equilibrium constant K_0. For a 90% reduction of the low pH current, the model predicts a concomitant >80% reduction in the capsaicin response, although the proton-potentiated response may stay approximately unchanged.

Several lines of evidence suggest that the pore of TRPV1 has an overall folding similar to that of K^+ channels. Mutagenesis study in the pore region of TRPV1 produce functional changes in the permeation properties as expected (Garcia-Martinez et al., 2000). Cysteine accessibility experiments on a related homolog, TRPV5, support a coil structure followed by a helical segment and two distinct coiled fragments before S6 (Dodier et al., 2004). The present study also shows a close homology in the pore sequences after removal of 15 residues. According to the KcsA structure (Doyle et al., 1998), T633 is located toward the N terminus of the putative pore helix. This region of the pore helix may interact with the top of S6 from the neighboring subunit as well as the turret (Fig. 2*F*). However, the exchange of the turret, which is least conserved in the TRPV family, showed little effect on the function of the channel. The mutagenesis experiment also revealed that the size, not the polarity, of T633 is important for its function, whereas the turret region is relatively hydrophilic. Thus, it is tempting to postulate that T633 may form hydrophobic interactions with the N terminus of S6 (Fig. 2*F*). If S6 forms the gate of TRPV1 as suggested in other channels, such an interaction may be necessary to stabilize pore opening, which would be consistent with our single-channel observations in which the opening events were dramatically shortened in the mutant.

The pore helix has been implicated in gating in several other ion channels containing a KcsA-like pore. In particular, the C terminus of the pore helix has been shown to dictate the stability of the open states and the duration of bursting activity in Kir channels (Alagem et al., 2003). The pore helix of Shaker K^+ channels is also involved in the C-type inactivation (Yang et al., 1997). In CNG channels, the pore helix residues show state-dependent accessibility to cysteine-modifying reagents depending on whether the channel is closed or open (Becchetti et al., 1999; Liu and Siegelbaum, 2000). Similar observations were reported in Ca^{2+}-selective TRPV5 channels (Yeh et al., 2005). However, relatively uncertain from these studies is whether the pore helix is collaterally or causally involved in channel opening. The present study demonstrates an explicit role of the pore helix in channel gating, and importantly, only for the activation by low pH. The capability to perturb the pore function in a stimulus-dependent manner should further help the investigation of the structural mechanisms of the pore conformational changes in these channels.

The S3–S4 linker of TRPV1 shows an unexpected critical role in the function of the channel. Other ion channels with six transmembrane domains such as the Shaker K^+ channel are tolerant to large deletions in the loop (Gonzalez et al., 2000). The discrepancy may suggest possible differences in the structures of these channels. The critical residue V538 appeared to reside at a strategic position; it is preceded by highly polar residues and followed by a proline and subsequently nonpolar residues. This arrangement suggests that the residue may be located at the interface between the solvent and lipid, making it susceptible to interactions with other hydrophobic residues. The S3 and S4 domains of TRPV1 have been implicated in vanilloid agonist binding (Chou et al., 2004; Gavva et al., 2004). In particular, the residue M547 is near the extracellular side of the S4 domain, and is required for RTX binding but not for capsaicin sensitivity (Chou et al., 2004). The proximity of the residue to V538 raises the question whether V538 is also involved in RTX activation. If RTX invokes a combination of structural changes for both proton and capsaicin activation, it would help explain the high potency of the compound. It is possible that the S3 and S4 domains of the channel undergo conformational changes common to all stimuli, but coupled to proton sensor activation through residues near the extracellular side, which would be consistent with both our observation on the selective effect of the linker on proton activation and also the involvement of S3 and S4 in capsaicin and RTX activations.

References

Alagem N, Yesylevskyy S, Reuveny E (2003) The pore helix is involved in stabilizing the open state of inwardly rectifying K^+ channels. Biophys J 85:300–312.

Baumann TK, Martenson ME (2000) Extracellular protons both increase the activity and reduce the conductance of capsaicin-gated channels. J Neurosci 20:RC80(1–5).

Baumann TK, Burchiel KJ, Ingram SL, Martenson ME (1996) Responses of adult human dorsal root ganglion neurons in culture to capsaicin and low pH. Pain 65:31–38.

Becchetti A, Gamel K, Torre V (1999) Cyclic nucleotide-gated channels. Pore topology studied through the accessibility of reporter cysteines. J Gen Physiol 114:377–392.

Bevan S, Docherty RJ (1993) Cellular mechanisms of the action of capsaicin.

In: Capsaicin in the study of pain (Wood JN, ed), pp 27–44. San Diego: Academic.

Bevan S, Yeats J (1991) Protons activate a cation conductance in a subpopulation of rat dorsal root ganglion neurones. J Physiol (Lond) 433:145–161.

Caterina MJ, Schumacher MA, Tominaga M, Rosen TA, Levine JD, Julius D (1997) The capsaicin receptor: a heat-activated ion channel in the pain pathway. Nature 389:816–824.

Caterina MJ, Rosen TA, Tominaga M, Brake AJ, Julius D (1999) A capsaicin-receptor homologue with a high threshold for noxious heat. Nature 398:436–441.

Caterina MJ, Leffler A, Malmberg AB, Martin WJ, Trafton J, Petersen-Zeitz KR, Koltzenburg M, Basbaum AI, Julius D (2000) Impaired nociception and pain sensation in mice lacking the capsaicin receptor. Science 288:306–313.

Chou MZ, Mtui T, Gao YD, Kohler M, Middleton RE (2004) Resiniferatoxin binds to the capsaicin receptor (TRPV1) near the extracellular side of the S4 transmembrane domain. Biochemistry 43:2501–2511.

Davis JB, Gray J, Gunthorpe MJ, Hatcher JP, Davey PT, Overend P, Harries MH, Latcham J, Clapham C, Atkinson K, Hughes SA, Rance K, Grau E, Harper AJ, Pugh PL, Rogers DC, Bingham S, Randall A, Sheardown SA (2000) Vanilloid receptor-1 is essential for inflammatory thermal hyperalgesia. Nature 405:183–187.

Dodier Y, Banderali U, Klein H, Topalak O, Dafi O, Simoes M, Bernatchez G, Sauve R, Parent L (2004) Outer pore topology of the ECaC-TRPV5 channel by cysteine scan mutagenesis. J Biol Chem 279:6853–6862.

Doyle DA, Morais CJ, Pfuetzner RA, Kuo A, Gulbis JM, Cohen SL, Chait BT, MacKinnon R (1998) The structure of the potassium channel: molecular basis of K^+ conduction and selectivity. Science 280:69–77.

Garcia-Martinez C, Morenilla-Palao C, Planells-Cases R, Merino JM, Ferrer-Montiel A (2000) Identification of an aspartic residue in the P-loop of the vanilloid receptor that modulates pore properties. J Biol Chem 275:32552–32558.

Gavva NR, Klionsky L, Qu Y, Shi L, Tamir R, Edenson S, Zhang TJ, Viswanadhan VN, Toth A, Pearce LV, Vanderah TW, Porreca F, Blumberg PM, Lile J, Sun Y, Wild K, Louis JC, Treanor JJ (2004) Molecular determinants of vanilloid sensitivity in TRPV1. J Biol Chem 279:20283–20295.

Gonzalez C, Rosenman E, Bezanilla F, Alvarez O, Latorre R (2000) Modulation of the Shaker K^+ channel gating kinetics by the S3–S4 linker. J Gen Physiol 115:193–208.

Guex N, Peitsch MC (1997) SWISS-MODEL and the Swiss-PdbViewer: an environment for comparative protein modeling. Electrophoresis 18:2714–2723.

Hui KY, Liu BY, Qin F (2003) Capsaicin activation of the pain receptor, VR1: multiple open states from both partial and full binding. Biophys J 84:2957–2968.

Jordt SE, Tominaga M, Julius D (2000) Acid potentiation of the capsaicin receptor determined by a key extracellular site. Proc Natl Acad Sci USA 97:8134–8139.

Klionsky L, Tamir R, Holzinger B, Bi X, Talvenheimo J, Kim H, Martin F, Louis JC, Treanor JJ, Gavva NR (2006) A polyclonal antibody to the prepore loop of transient receptor potential vanilloid type 1 blocks channel activation. J Pharmacol Exp Ther 319:192–198.

Kress M, Fetzer S, Reeh PW, Vyklicky L (1996) Low pH facilitates capsaicin responses in isolated sensory neurons of the rat. Neurosci Lett 211:5–8.

Kuzhikandathil EV, Wang H, Szabo T, Morozova N, Blumberg PM, Oxford GS (2001) Functional analysis of capsaicin receptor (vanilloid receptor subtype 1) multimerization and agonist responsiveness using a dominant negative mutation. J Neurosci 21:8697–8706.

Liu B, Hui K, Qin F (2003) Thermodynamics of heat activation of single capsaicin ion channels VR1. Biophys J 85:2988–3006.

Liu B, Ma W, Ryu S, Qin F (2004) Inhibitory modulation of distal C-terminal on protein kinase C-dependent phospho-regulation of rat TRPV1 receptors. J Physiol (Lond) 560:627–638.

Liu J, Siegelbaum SA (2000) Change of pore helix conformational state upon opening of cyclic nucleotide-gated channels. Neuron 28:899–909.

Martenson ME, Ingram SL, Baumann TK (1994) Potentiation of rabbit trigeminal responses to capsaicin in a low pH environment. Brain Res 651:143–147.

Petersen M, Lamotte RH (1993) Effect of protons on the inward current evoked by capsaicin in isolated dorsal root ganglion cells. Pain 54:37–42.

Ryu SJ, Liu BY, Qin F (2003) Low pH potentiates both capsaicin binding and channel gating of VR1 receptors. J Gen Physiol 122:45–61.

Simone DA, Baumann TK, Collins JG, Lamotte RH (1989) Sensitization of cat dorsal horn neurons to innocuous mechanical stimulation after intradermal injection of capsaicin. Brain Res 486:185–189.

Steen KH, Reeh PW (1993) Sustained graded pain and hyperalgesia from harmless experimental tissue acidosis in human skin. Neurosci Lett 154:113–116.

Tominaga M, Caterina MJ, Malmberg AB, Rosen TA, Gilbert H, Skinner K, Raumann BE, Basbaum AI, Julius D (1998) The cloned capsaicin receptor integrates multiple pain-producing stimuli. Neuron 21:531–543.

Welch JM, Simon SA, Reinhart PH (2000) The activation mechanism of rat vanilloid receptor 1 by capsaicin involves the pore domain and differs from the activation by either acid or heat. Proc Natl Acad Sci USA 97:13889–13894.

Yang Y, Yan Y, Sigworth FJ (1997) How does the W434F mutation block current in Shaker potassium channels? J Gen Physiol 109:779–789.

Yeh BI, Kim YK, Jabbar W, Huang CL (2005) Conformational changes of pore helix coupled to gating of TRPV5 by protons. EMBO J 24:3224–3234.